Research Paper

A cyclic-RGD-BioShuttle functionalized with TMZ by DAR$_{inv}$ "Click Chemistry" targeted to $\alpha_v\beta_3$ integrin for therapy

Klaus Braun[1]* ✉, Manfred Wiessler[1]*, Rüdiger Pipkorn[2], Volker Ehemann[3], Tobias Bäuerle[1], Heinz Fleischhacker[1], Gabriele Müller[4], Peter Lorenz[1], Waldemar Waldeck[4]

1. German Cancer Research Center, Dept. of Imaging and Radiooncology, INF 280, D-69120 Heidelberg, Germany
2. German Cancer Research Center, Central Peptide Synthesis Unit, INF 580, D-69120 Heidelberg, Germany
3. University of Heidelberg, Institute of Pathology, INF 220, D-69120 Heidelberg, Germany
4. German Cancer Research Center, Division of Biophysics of Macromolecules, INF 580, D-69120 Heidelberg, Germany

* The authors contributed equally to this work

✉ Corresponding author: Klaus Braun, Ph.D., German Cancer Research Center (DKFZ), Dept. of Imaging and Radiooncology, Im Neuenheimer Feld 280, D-69120 Heidelberg, Germany. Phone: +49 6221-42 2495; Fax: +49 6221-42 3326; e-mail: k.braun@dkfz.de

Abstract

Clinical experiences often document, that a successful tumor control requires high doses of drug applications. It is widely believed that unavoidable adverse reactions could be minimized by using gene-therapeutic strategies protecting the tumor-surrounding healthy tissue as well as the bone-marrow. One new approach in this direction is the use of "Targeted Therapies" realizing a selective drug targeting to gain effectual amounts at the target site, even with drastically reduced application doses. MCF-7 breast cancer cells expressing the $\alpha_v\beta_3$ [alpha(v)beta(3)] integrin receptor are considered as appropriate candidates for such a targeted therapy. The modularly composed BioShuttle carrier consisting of different units designed to facilitate the passage across the cell membranes and for subcellular addressing of diagnostic and/or therapeutic molecules could be considered as an eligible delivery platform. Here we used the cyclic RGD-BioShuttle as a carrier for temozolomide (TMZ) at the $\alpha_v\beta_3$ integrin receptor realizing local TMZ concentrations sufficient for cell killing. The IC50 values are 12 µMol/L in the case of cRGD-BioShuttle-TMZ and 100 µMol/L for underivatized TMZ, which confirms the advantage of TMZ reformulation to realize local concentrations sufficient for cell killing.

Our paper focuses on the design, synthesis and application of the cRGD-BioShuttle conjugate composed of the cyclic RGD, a $\alpha_v\beta_3$ integrin-ligand, ligated to the cytotoxic drug TMZ. The ligation was carried out by the Diels Alder Reaction with inverse electron demand (DAR$_{inv}$).

Key words: Click-Chemistry, Cycloaddition, BioShuttle, Ligation chemistry, Linker Systems, Adaptor Systems, inverse Diels Alder Reaction, RGD, Tetrazines, targeted Therapy, Temozolomide

Introduction

Breast cancer is one of the most common malignancies affecting women in developed countries.[1] Approximately three out of four women with breast cancer develop metastases in bone which, in turn, diminish the quality of life.[2] An optimal treatment concept for patients needs different therapy modalities and methods with an optimum in efficiency and the greatest possible protection. Attention should be

laid on an individual and not just standardized plan of treatment for every single patient and all available therapy options should be used, such as immunotherapy, surgery or chemotherapy sensibly using cytostatic active agents with acceptable adverse reactions. It is remarkable how dated medical treatment methods are persistently continued [reported during the "International Brain Tumor Research Conference 2010 (http://www.kgu.de/index.php?id=4290)].

Toxic side effects are documented for TMZ as adverse reactions in the bone-marrow. Moreover, it is known from clinical experience, that even higher application doses are necessary for successful tumor control. This approach seems obsolete now, because 'Targeted Therapy' has reached the focus of scientific interest in order to minimize such unavoidable drastic side effects. Strategies were discussed during the aforementioned meeting to protect the bone-marrow, e.g. with gene-therapeutic methods. Another interesting field is the regional chemotherapy in which cytostatic drugs are being locally applied to certain body regions. The topical application increases the amount of active substances in the tumor and improves efficiency, while lowering the side effect rate at the same time.

However, many cell immanent obstacles inhibit chemical therapy, such as the multidrug resistance (MDR) mediated against cytotoxic agents like TMZ, and apoptosis resistance with disruption of the complex programmed cell death pathway network. The Janicke group documented apoptosis resistant MCF-7 breast cancer cells treated with ionizing radiation, however especially breast micro-metastases are difficult to determine and even more difficult to treat effectively.

Therefore only a selective targeting of the drug can deliver an effectual amount of TMZ to its target site, even with drastically reduced application doses. How to perform this is exemplarily shown here by targeting and controlling breast cancer cells.

Our considerations to overcome these resistance-inducing factors led to the application of ligands, which are target-specific for cell-typical surface receptors, as described as follows.

On these cells the $\alpha_v\beta_3$ [alpha(v)beta(3)] and $\alpha_v\beta_5$ [alpha(v)beta(5)]integrins are heterodimeric cell surface receptors which mediate adhesion between cells and the extracellular matrix.[3] The $\alpha_v\beta_3$ receptor has previously been implicated in a key role of tumor progression, metastasis and osteoclast bone resorption. [4] Integrins, the corresponding ligands, are evolutionarily old and have critical roles during developmental and pathological processes. The antibodies to $\alpha_v\beta_3$ integrin and its antagonists like

arg-gly-asp (RGD)-containing peptides, including osteopontin, bone sialoprotein, vitronectin and fibrinogen are considered as efficient inhibitors which can control the tumor progression.[5]

This $\alpha_v\beta_3$ integrin receptor is documented as an outstanding target in the field of tumor imaging [6-8] and is equally important as a chemotherapeutic target in the field of targeted therapy.[9]

Endocytosis-mediated intracellular trafficking of ligands via the $\alpha_v\beta_3$ receptor of MCF-7 cells and the $\alpha_v\beta_5$ integrin receptor into the perinuclear region of HeLa cells is documented, which lack the functional $\alpha_v\beta_3$ receptor.[10] Interestingely HeLa cells, which express the $\alpha_v\beta_3$ integrin receptor at low level, possess lower invasive potential than MCF-7 cells. In our experiments we used MCF-7 human breast cancer cells and HeLa cervix cancer cells to investigate the new cRGD-BioShuttle as a delivery platform for targeting with TMZ in order to realize high local TMZ concentrations at the MCF-7 and HeLa cell's surfaces and, after uptake into the cells sufficient for cell killing.

This paper intends to summarize the major efforts reached thus far and focuses on the design, synthesis and application of the cRGD-BioShuttle-TMZ conjugate. The whole molecule was synthesized via Diels Alder Reaction with inverse electron demand. It is composed of the cyclic RGD-containing the $\alpha_v\beta_3$ and $\alpha_v\beta_5$ integrin antagonist cRGD.

Cell culture

The estrogen sensitive MCF-7 adenocarcinoma breast cancer and HeLa cervix cancer cells (dkfz, tumorbank) were maintained at 37°C in a 5% CO_2 atmosphere in RPMI cell medium (Gibco, Germany) supplemented with 5% fetal calf serum (Biochrome, Germany). The cells were split twice a week.

Chemical Procedures

Synthesis of the RGD-BioShuttle

Derivatization of temozolomide

N-(2-Aminopropyl)-4-(6-(pyrimidine-2-yl)-1,2,4,5-tetrazine-3-yl)benzamide 4

4-(6-(Pyrimidine-2-yl)-1,4-dihydro-1,2,4,5-tetrazine-3-yl)benzoic acid (**3**) was prepared from 2-cyanopyrimidine **1** and 4-cyano-benzoic acid **2** by reaction with hydrazine and then oxidized with sodium nitrite to the tetrazine derivative **4** according to the following procedure [11]. The tetrazine derivative was converted with thionyl chloride under standard conditions to the chloride **5**. To this suspension of the acid chloride (2 mmol) in 20 ml CH_2Cl_2 a solution of

N-Boc-1,3-diaminopropane (2 mmol) and TEA (2 mmol) in 10 ml CH$_2$Cl$_2$ was slowly added at 0-5°C. The resulting solution was deeply coloured and maintained for 4 h at room temperature. Then the organic phase was washed with water, followed by 1N HCl and again water. The organic layer was dried over Na$_2$SO$_4$ and evaporated. The resulting residue was chromatographed on silica gel by elution with chloroform/ethanol (9:1) and further purified by re-crystallization from acetone. Yield: 50 to 70 % depending on the quality of the carboxylic acid. ESI MS: *m/z* 437.2 [M]$^+$. The Boc-protected derivative was treated with TFA (5 ml) for 30 min at room temperature and isolated by evaporation to a solid residue (**6**) (ESI: *m/z* 337.2 [M]$^+$ (as shown in Figure A).

rated under vacuum and the resulting solid was stored over NaOH.

3-Methyl-4-oxo-*N*-(3-(4-(6-(pyrimidine-2-yl)-1,2,4,5-tetrazine-3-yl) benzamido)propyl)-3,4-dihydroimidazo[5,1-d][1,2,3,5]tetrazine-8-carboxamide (TMZ-tetrazine diene) 9

Compound **8** (0.5 mmol) and the chloride **7** (0.5 mmol) were dissolved in 5 ml chloroform and 5 ml TEA at 0-5 °C. After 4 h at room temperature, the solution was washed with water, 1 N HCl and again with water. The organic layer was dried over Na$_2$SO$_4$ and evaporated. The residue was purified by chromatography (silica gel) with chloroform/ethanol (9.5/0.5). Yield: 68%: ESI: *m/z* 536.3 [M+Na]$^+$. (Figure B)
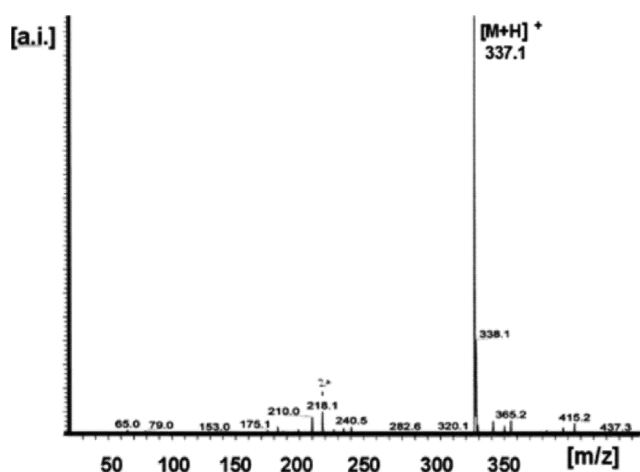

Figure A shows the mass of the *N*-(2-Aminopropyl)-4-(6-(pyrimidine-2-yl)-1,2,4,5-tetrazine-3-yl)benzamide (**6** in scheme 1/Figure S1), as discussed by Wiessler [12].
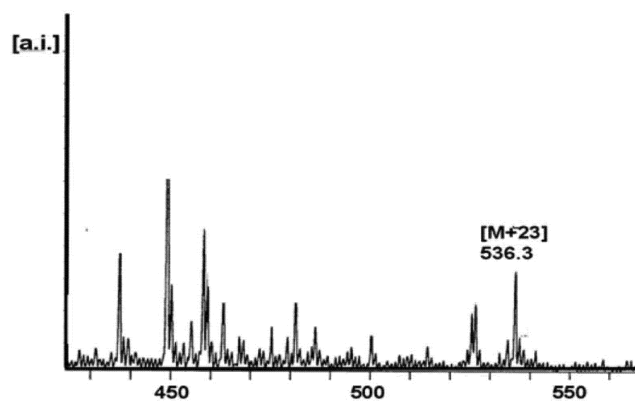

Figure B shows the mass of 3-methyl-4-oxo-*N*-(3-(4-(6-(pyrimidine-2-yl)-1,2,4,5-tetrazine-3-yl)benzamido)propyl)-3,4-dihydroimidazo[5,1-d][1,2,3,5]tetrazine-8-carboxamide {TMZ-tetrazine diene (**9** in scheme 1/Figure S1)} [12].

3-Methyl-4-oxo-3,4-dihydroimidazo[5,1-d][1,2,3,5]tetrazine-8-carboxylic acid chloride 7

3-Methyl-4-oxo-3,4-dihydroimidazo[5,1-d][1,2,3,5]tetrazine-8-carboxylic acid was converted to the corresponding chloride **7** as documented by Arrowsmith [13]. The acid (2 mmol) was refluxed with thionyl chloride (10 ml) until the acid was completely dissolved. The excess of thionyl chloride was evapo-

Derivatizations of the cRGD

Synthesis of the Reppe anhydride 12

The tetracyclo-[5.4.2^{1,7}.0^{2,6}.0^{8,11}]3,5-dioxo-4-aza-9,12-tridecadiene (Reppe-anhydride) **12** was prepared from 42 mg of (1Z,3Z,5Z,7Z)-cycloocta-1,3,5,7-tetraene **10** and 44 mg maleic anhydride **11** in chloroform as documented by Reppe [14].
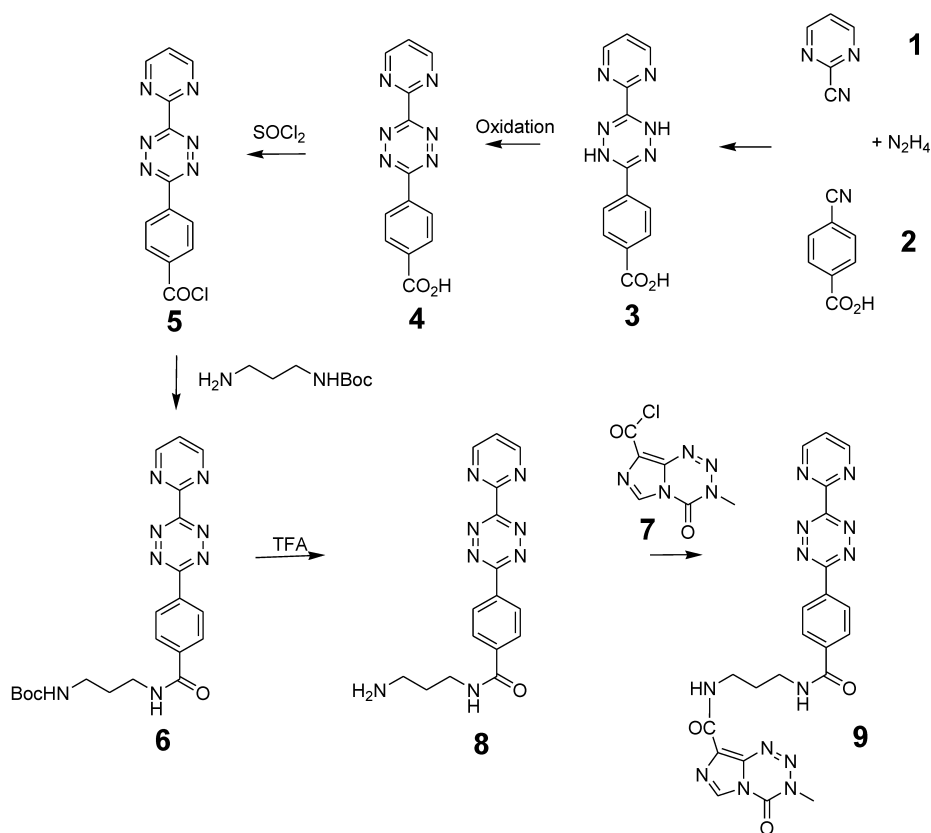
Figure S1 (Scheme 1) the nitriles 1 and 2 react with hydrazine to the 4-(6-(pyrimidine-2-yl)-1,4-dihydro-1,2,4,5-tetrazine-3-yl)benzoic acid 3. Oxidation to 4 and reaction with thionyl chloride result in the corresponding acide chloride 5 which reacts with *N*-Boc-1,3-diaminopropane to the product 6. Boc-deprotection and subsequent reaction with 3-Methyl-4-oxo-3,4-dihydroimidazo[5,1-d][1,2,3,5]tetrazine-8-carboxylic acid chloride 7 result in the product 3-Methyl-4-oxo-*N*-(3-(4-(6-(pyrimidine-2-yl)-1,2,4,5-tetrazin-3-yl)benzamido)propyl)-3,4-dihydroimidazo[5,1-d][1,2,3,5]tetrazine-8-carboxamide (TMZ-tetrazine diene) 9.
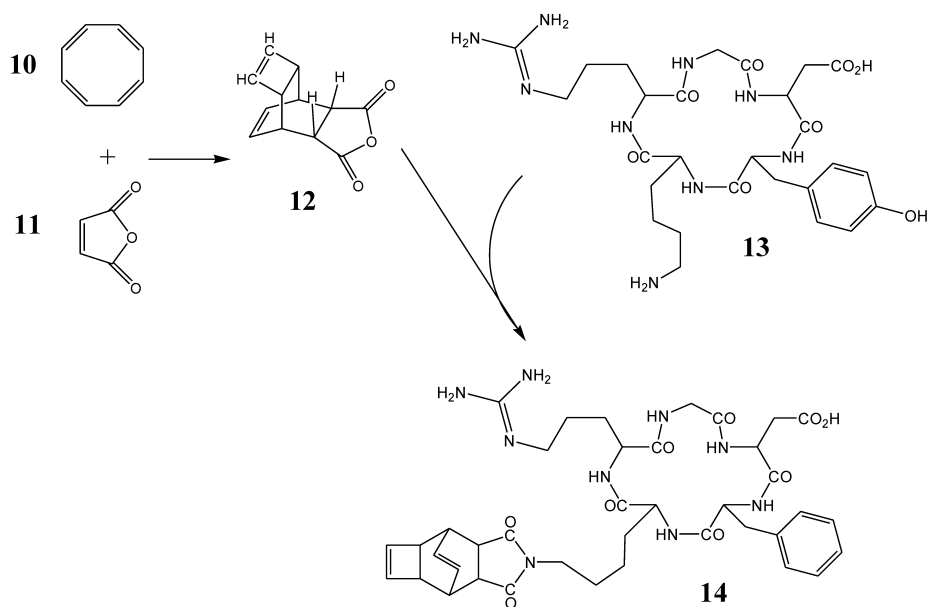
Figure S2 (Scheme 2) illustrates the chemical reaction of (1Z,3Z,5Z,7Z)-cycloocta-1,3,5,7-tetraene 10 and 44 mg maleic anhydride 11 which produces the tetracyclo-[5.4.2^{1,7}.0^{2,6}.0^{8,11}]-3,5-dioxo-4-aza-9,12-tridecadiene 14 (NMH data of 12 are shown in the Figure C.
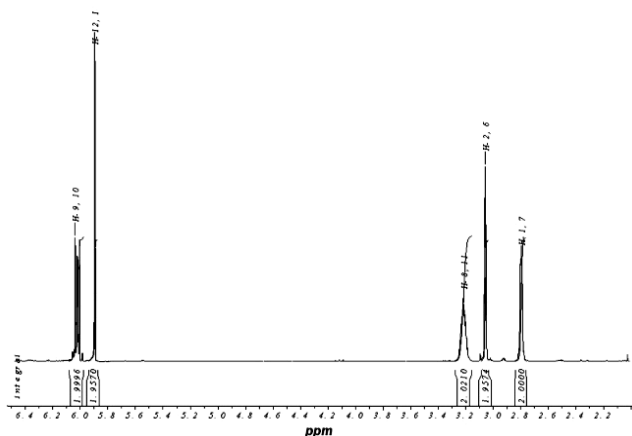
Figure C shows the ¹H-NMR-spectrum of the Reppe Anhydride {TcT = (Tetracyclo-[5.4.2¹,⁷.O²,⁶.O⁸,¹¹] 3,5-dioxo-4-aza-9,12-tridecadiene in CDCl₃}. The structure describes the shift calculation for protons of the compound with ChemDraw Ultra 2004. (Numbers indicate the predicted shift of the signals in ppm, as discussed by Wiessler [12].

Synthesis of the dienophile cRGD-Lys(Tct) (14)

30 µmol cRGD peptide (18 mg) **13** and 40 µmol (8 mg) tetracyclo-[5.4.2^{1,7}.0^{2,6}.0^{8,11}]3,5-dioxo-4-aza-9,12-tridecadiene **12** were dissolved in pyridine over 5 hours at 70° - 80°C. Yield: 6 mg **14**. Empirical formula C39H49N9O9; exact Mass: 787.37 Mol. Wt.: 787.86

m/e: 787,37 (100,0%), 788,37 (43,1%), 789,37 (12,3%), 788,36 (3,3%), 790,38 (1,2%), 790,37 (1,1%) C, 59.45; H, 6.27; N, 16.00; O, 18.28 m/e peak at 788.5 for the product.

Ligation of the cRGD-Lys(Tct) with the TMZ-tetrazine 9

Equimolar amounts of the TMZ-tetrazine conjugate **9** (1.03 mg; 2 µmol) and cRGD-Lys(Tct) **14** (7.3 mg, 2 µmol) were dissolved in aqueous solution and stored at room temperature for 24 h. The DAR$_{inv}$ reaction occurs at room temperature and was completed after the colour changed from magenta to yellow. The product **15** (cRGD-BioShuttle-TMZ) was isolated by lyophilization; yield: 98 %); MS ESI: *m/e* 1634.8; calculated C81H91N19O15S2 1633.6.

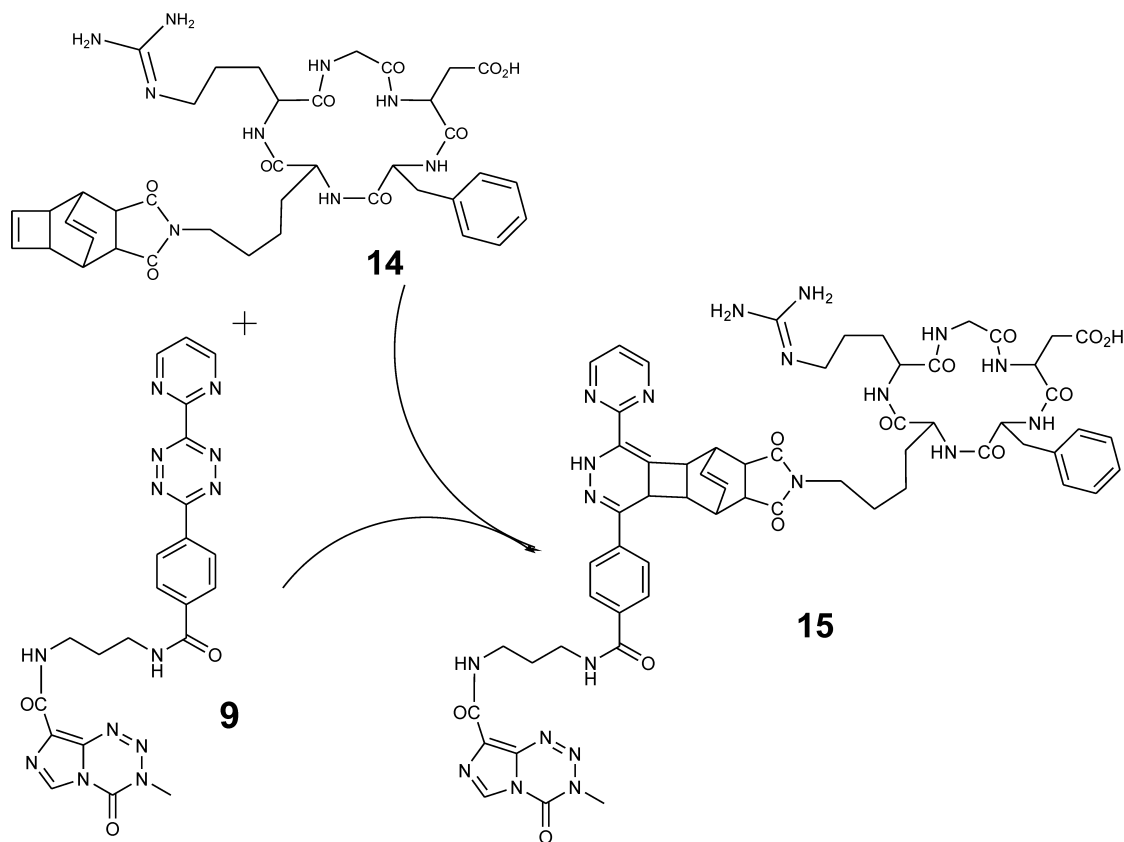**Figure S3** (Scheme 3) shows the DAR$_{inv}$ reaction of the diaryl-tetrazine harbouring TMZ 9 with cRGD functionalized with the Reppe Anhydride 14 to the product 15 (cRGD-BioShuttle-TMZ).

Synthesis of the cRGD-dansyl

For investigations of the cellular localization of the cRGD we functionalized the cRGD with the fluo-rescent dye 5-(dimethylamino)-naphthalene-1-sulfonyl, (*dansyl,* as shown in scheme 4/Figure S4).
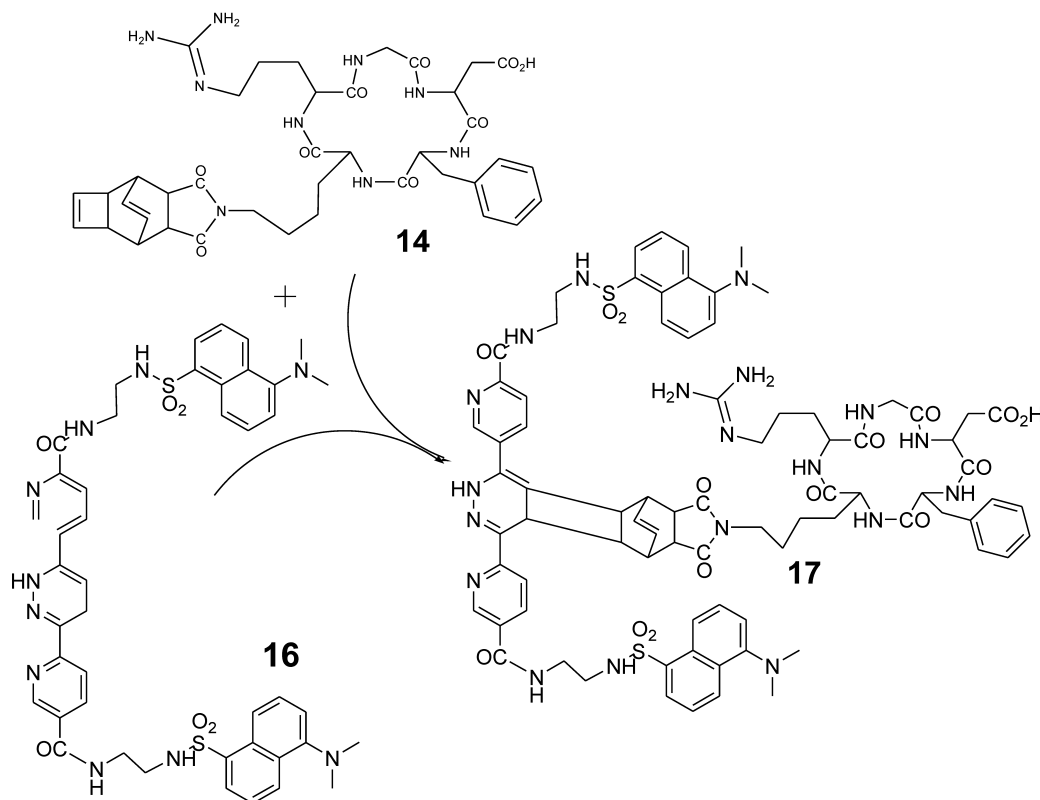

Figure S4 (Scheme 4) shows the DAR$_{inv}$ reaction of the diaryl-tetrazine harbouring the 5-(dimethylamino)-naphthalene-1-sulfonyl dye **16** with cRGD functionalized with the Reppe Anhydride **14** to the product **17** (cRGD-BioShuttle-dansyl).

Synthesis of the cRGD-dansyl 17

2 μmol (1.75 mg) of purified **14** reacts over 24 hours with 2.5 μmol (2.18 mg) **16** dissolved in DMSO at room temperature to the product **17**. The reaction mixture was concentrated. After HPLC purification the estimations of identity show in position 1634, Mode m/e.

Exact Mass: 1633.64; Mol. Wt.: 1634.84

m/e: 1633.64 (100.0%), 1634.64 (97.8%), 1635.65 (39.3%), 1636.65 (14,2%), 1636.64 (11.9%), 1635.64 (10.8%), 1635.63 (9.4%), 1637.65 (4,7%), 1637.64 (4,2%), 1638.64 (1.6%)

C, 59.51; H, 5.61; N, 16.28; O, 14.68; S, 3.92

Chemotherapy treatment of MCF-7 breast cancer and HeLa cervix cancer cells

Pure temozolomide (TMZ) [Sigma-Aldrich, Germany (Cat. No. 76899)] was subdivided into two parts for subsequent processing. One part was kept underivatized for the following experiment and the second part, after chemical transformation to the cor-responding acid chloride **7**, was used for coupling to the cRGD [Peptides International, USA (Cat. No. PCI-3661-PI)] transporter molecule.

TMZ and cRGD-BioShuttle-TMZ **15** were both dissolved in 10 % aqueous solution of acetonitrile (Sigma-Aldrich, Germany). Control studies with ace-tonitrile were performed to exclude potential toxic effects of this solvent.

MCF-7 and HeLa cells were grown as subcon-fluent monolayers in RPMI (control) and in RPMI containing appropriate amounts of TMZ and the cRGD-BioShuttle-TMZ **15** (50 μM) and their behav-iour was analyzed for up to 72 hours.

Morphological evaluation

Microscopical studies of the human cancer cells were carried out with an Olympus inverted micro-scope under phase contrast conditions. The magnifi-cation was 200fold. The cells were observed during their culture in medium and during treatment with the different drugs.

Cellular localization of the cRGD-BioShuttle-dansyl

In order to reconfirm our data documenting an endocytotic internalization of the cRGD into the cytoplasm of $\alpha_v\beta_3$ and $\alpha_v\beta_5$ integrin expressing cells we used the confocal laser scanning microscope (CLSM) of the Microscopy Core Facility of the German Cancer Research Center for qualified verification of the data. The pictures were taken with a Leica confocal microscope TCS SP5 II (excitation at 405 nm, emission at 420-560 nm) and examined with the Leica LAS-Software.

24 hours before CLSM measurements both cell lines, the HeLa and the MCF-7 cells (5×10^5), were cultivated in 8-well cell culture plates (Lab-Tek®) and treated with the cRGD-BioShuttle-dansyl (12.5 μM) **17**.

Cytotoxic Measurements

For the toxicological characterization of the cRGD-BioShuttle-TMZ conjugate **15** as well as the cRGD and the TMZ alone as controls were added to the MCF-7 cell line's medium. The substances were incubated in a dilution series ranging from 12.5, via 25, 50, to 100 μM final concentrations up to 72 hours. The IC50 values were determined and also converted to the pIC50 scale (-log IC50) (Table 1).

Multiparametric Flow Cytometry Analysis

Cell size and granularity

The use of the flow cytometry parameters forward (FSC) and sideward (SSC) scatter of the cells give an indication on drug effects through the relative cell size and structural effects such as granularity. Both parameters suffice for a rough cell characterization. The cells (treated with the components as described above and an untreated control) could be clearly distinguished as shown in the Figure 5.

Results

This manuscript details the synthetic steps of our new cRGD-BioShuttle-TMZ and illustrates the cellular uptake of this newly synthesized cRGD-BioShuttle-TMZ in comparison to its controls as outlined in the respective experiments. We examined MCF-7 and HeLa cells surface targeting of these molecules with the cytotoxic drug TMZ as a cargo.

Light Microscopical Studies

In light microscopy we first investigated the cell killing effect of cRGD-Bioshuttle-TMZ **15** compared to underivatized TMZ. We achieved a rapid and high local concentration and an accumulation of TMZ on the surface of the targeted $\alpha_v\beta_3$ integrin expressing MCF-7 cells by use of the cRGD-BioShuttle as delivery and targeting platform.

Figure 1 reveals the different effects of TMZ and cRGD-BioShuttle-TMZ on MCF-7 cells tested after 24 hours and 72 hours of treatment with a final concentration of 50 μM. Whereas the MCF-7 cells exhibit no formation of the squamous epithelium (**B**), the MCF-7 cells seem to be unimpressed by TMZ treatment (bottom row **C**) and resemble the untreated control (top row **A**) as shown in the microscopic pictures.

Figure 2 indicates a clear change of the MCF-7 phenotype dependent on the concentrations of cRGD-BioShuttle-TMZ of up to 50 μM. The untreated control cells are shown in the bottom row for each treatment regimen. The final concentrations of the cRGD-BioShuttle-TMZ and TMZ were from 12.5 μM, via 25 μM to 50 μM as indicated in the figure 2. A drastic cell killing of the MCF-7 cells was observed by the targeted approach, whereas the MCF-7 cells treated with underivatized temozolomide seemed to be not affected. Independent of the final TMZ concentrations used, they looked identical to the untreated control cells.

Cellular Localization Studies using Confocal Laser Scanning Microscopy – CLSM

In order to investigate the open question of the cellular localization of the cRGD-BioShuttle-TMZ we ligated a fluorescence dye to cRGD. This "BioShuttle" (cyclo RGD) connected to a fluorescent tag dansyl (as shown in scheme 4/Figure S4) was applied to the culture media of the $\alpha_v\beta_3$ and $\alpha_v\beta_5$ integrin expressing MCF-7 and the low expressing HeLa cells. The cells lines clearly show differences in the fluorescence signal localizations. Two hours after cRGD-BioShuttle-dansyl application a blue perinuclear dansyl fluorescence signal could be observed in MCF-7. The cell nucleus displayed no signal at all. The HeLa cells show a cells surface located fluorescence signal (Figure 3, top row).

24 hours after cRGD-BioShuttle-dansyl application the fluorescence signal increased in the cytoplasm of MCF-7 and at the surface of HeLa cells, but the signal localizations remained unaltered. A nuclear located fluorescence signal was still lacking (as shown in Figure 3, second row). The pictures from 48 and 72 hours after application demonstrate a decreased fluorescence signal suggesting an efflux of the dansyl fluorescence dye out of the MCF-7 cell's cytoplasm, whereas in contrast the fluorescence signal at the HeLa cell's surface is unchanged (Figure 3, row 3 and bottom row).

Cellular localization of the dansyl fluorochrome

For detailed information about the cellular localization of the dansyl fluorochrome 8 pictures of a z-stack were visualized in layers by CLSM. It is demonstrative, that some fluorescence signals are shown inside of the cells, but the signal is not only localized at the cell's surface but also detectable inside as pointed out in the legend of the figure 4.

Multiparametric FACS analysis

The morphological parameters of the FACS analysis shows an unaltered cell size (Figure 5, bottom row), whereas the granularity (influenced by size and structure of the cell nucleus and by the quantity of vesicles) is changed and shows an increased fraction of more granulized MCF-7 cells in all treatments (TMZ, cRGD, and cRGD-BioShuttle-TMZ) in contrast to the untreated MCF-7 control cells. As demonstrated in figure 5 the granularity of MCF-7 cells is increased in cells treated with TMZ and cRGD (100 µM respectively). The most conspicuous granularity was obtained after cRGD-BioShuttle-TMZ in the final concentration of 12.5 µM as shown in the blot of the figure 5 (right column, row 1).

The treatment of TMZ, cRGD, and cRGD-BioShuttle-TMZ in the concentrations as mentioned above shows no visible influence on the cell size of MCF-7 cells.
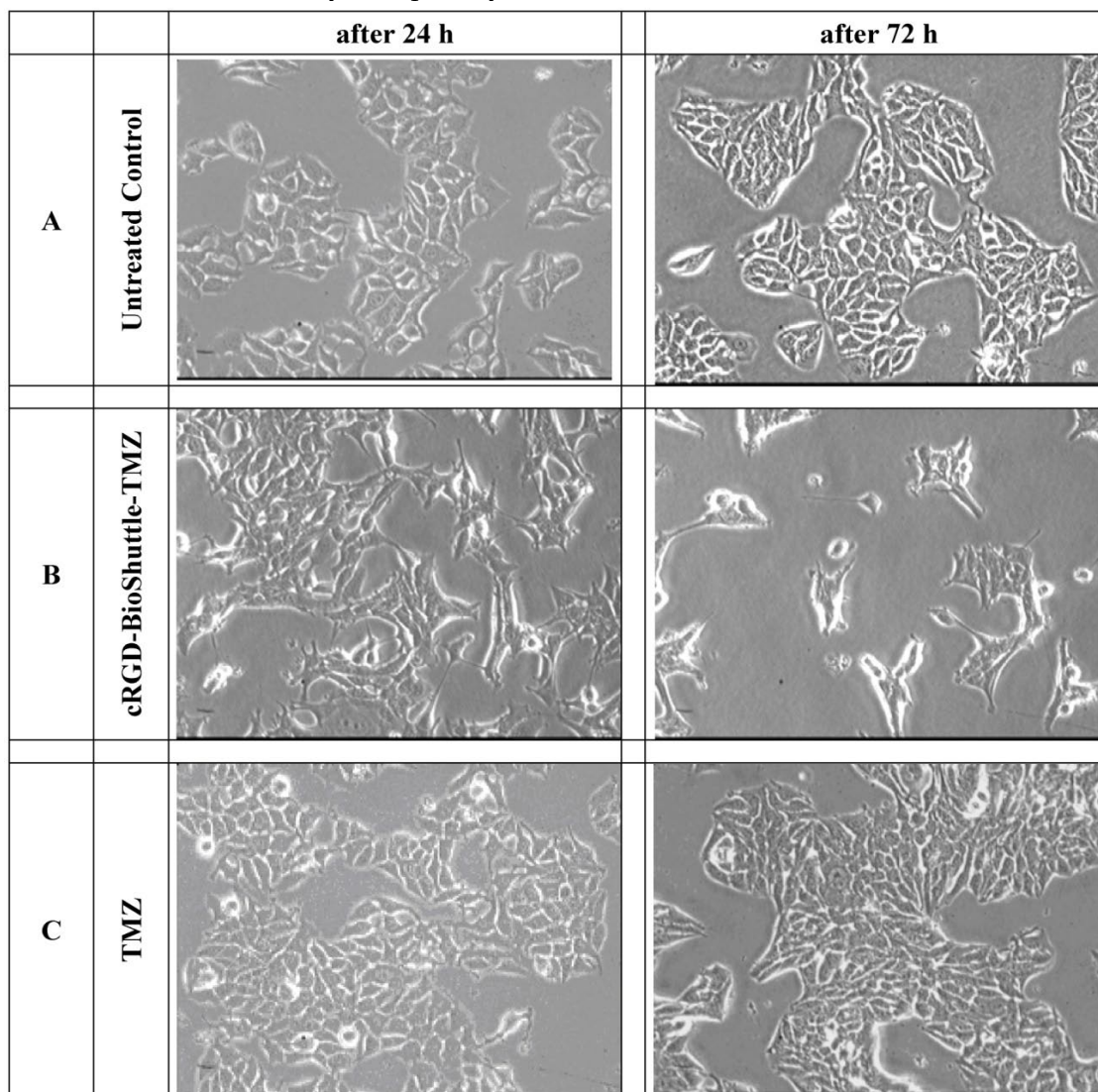

Figure 1　shows microscopical DIC studies of human breast cancer cells (MCF-7). The top row (A) shows the phenotype of untreated MCF-7 cells. The center row (B) exhibits MCF-7 cells after 24 hours (left column) and 72 hours (right column) of treatment with the cRGD-BioShuttle-TMZ 15 targeted to the MCF-7 cells surface arranged $\alpha_v\beta_3$ and $\alpha_v\beta_5$ integrins. MCF-7 cells treated with TMZ alone are shown in the bottom row (C). The final concentrations of the tested TMZ and cRGD-Bioshuttle-TMZ were 50 µM. The magnification was 200× with phase contrast.

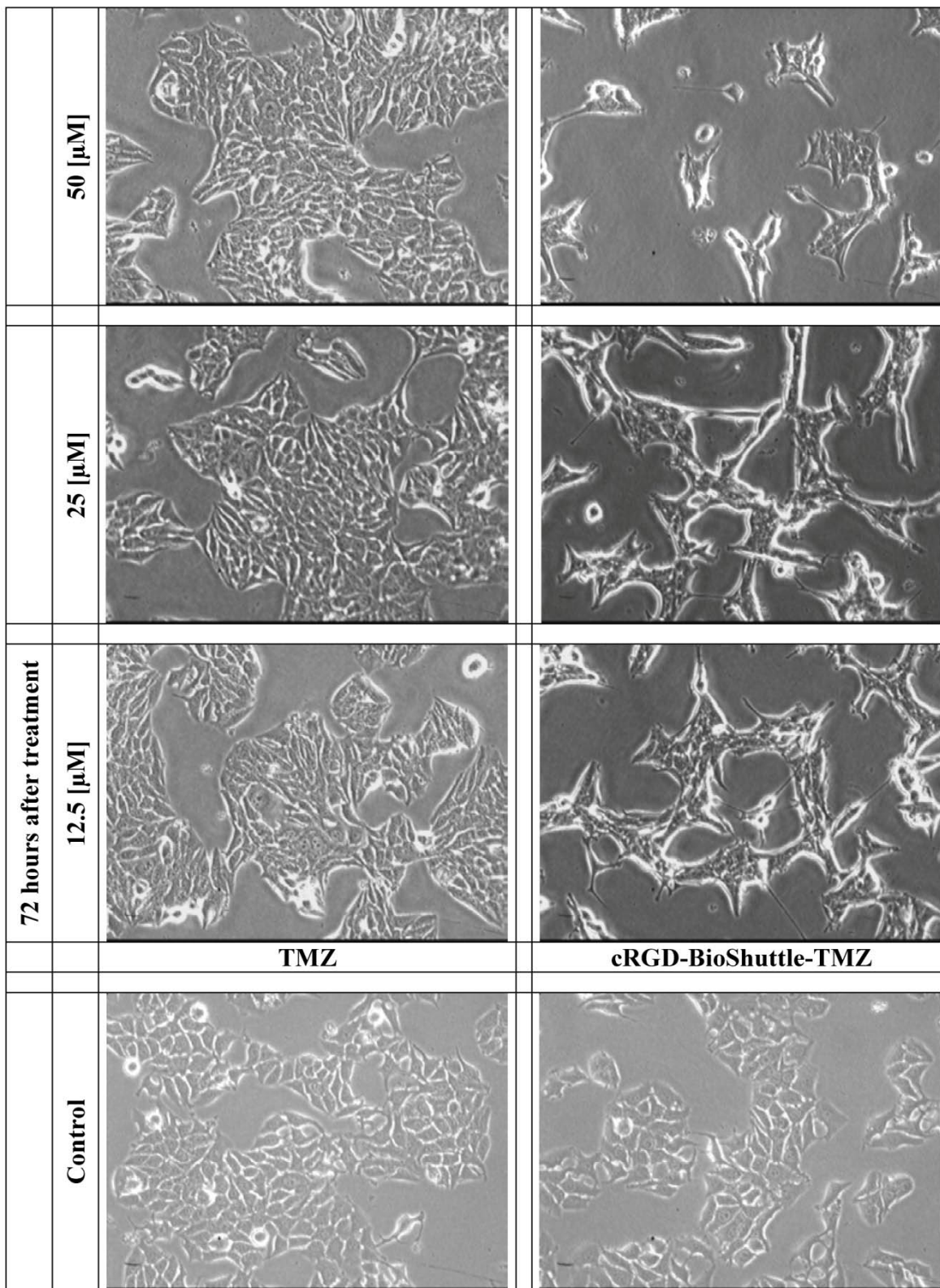**Figure 2**   illustrates the concentration dependent change of the phenotype of MCF-7 cells 72 hours after treatment with TMZ alone and cRGD-BioShuttle-TMZ. The left column represents the TMZ treatment; the untreated controls are at the lower end. The columns on the right side show treatment with the cRGD-BioShuttle-TMZ beginning with 50 μM via 25 μM to 12.5 μM.

Figure 3 The figure shows CLSM pictures of breast cancer cells MCF-7 (right column) and cervix cancer cells HeLa (left column). The lines of the figure indicate the measurement time points from 2h, 24h, 48h, up to 72h and suggest a different cellular localization of the cRGD-BioShuttle-dansyl molecule in both investigated cell lines. Two hours after cRGD-BioShuttle-dansyl application the molecule seems to be arrested on the surface of HeLa cells, whereas the dansyl-fluorescence can be observed in the cytoplasm of MCF-7 cells. 24 hours later and up to 72 hours, the localization of the fluorescence signal was unaltered on the surface of HeLa cells. The MCF-7 cells show a clear fluorescence signal in the cytoplasm except from cell nuclei which present no signal. From 48 to 72 hours after cRGD-BioShuttle-dansyl application the fluorescence signal in the MCF-7's cytoplasm diminishes increasingly. The final concentration of the cRGD-BioShuttle-dansyl was 50 µM.
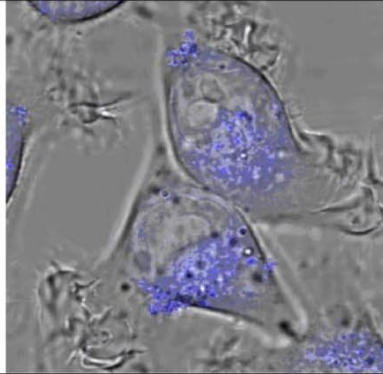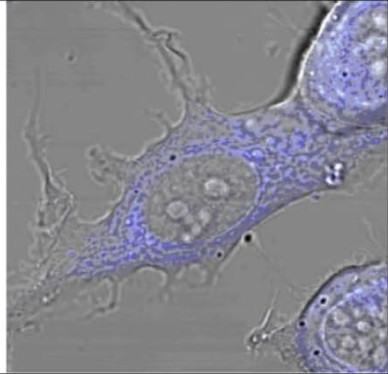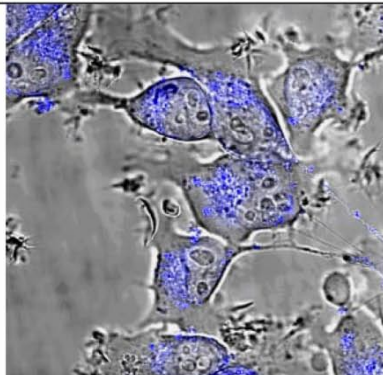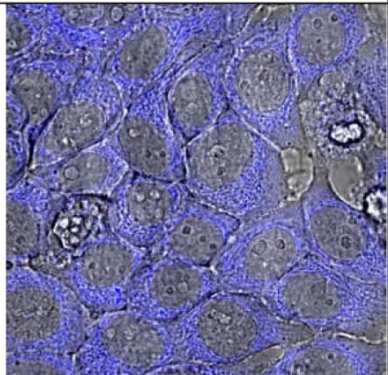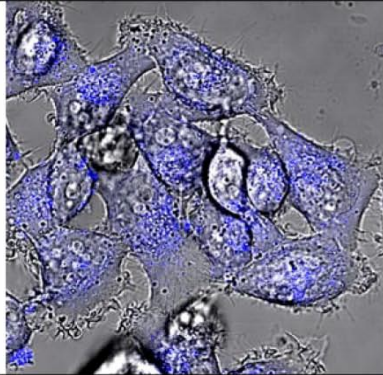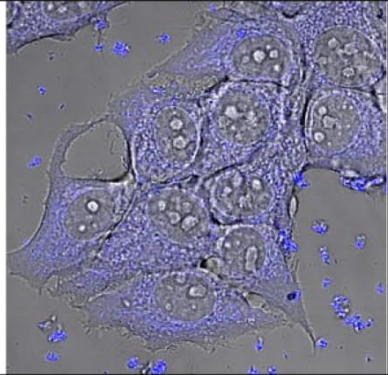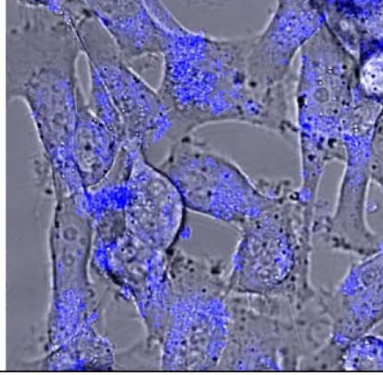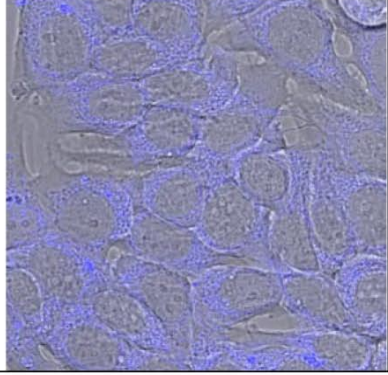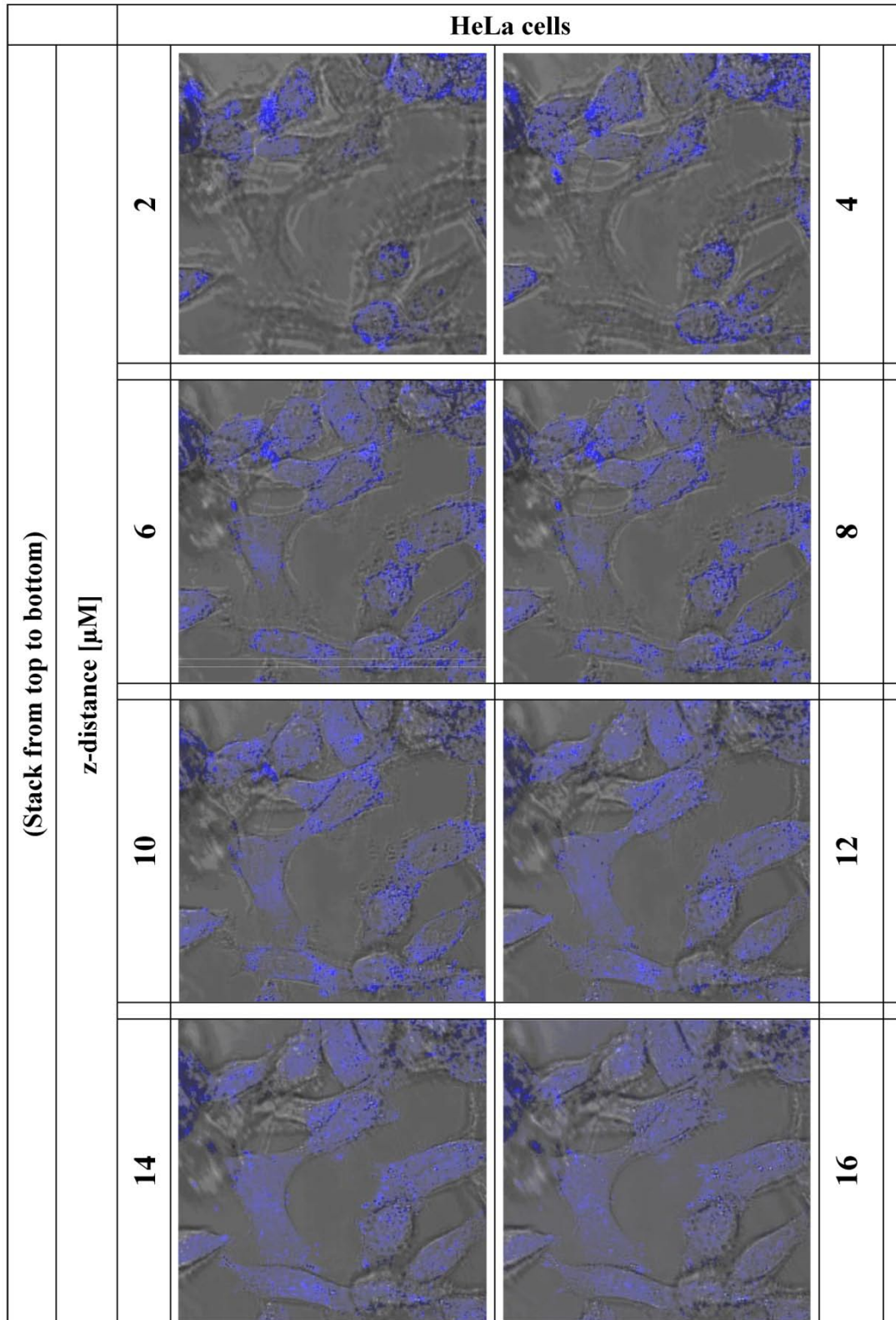
Figure 4   The gallery represents 8 CLSM pictures of treated HeLa cells in the x, y, and in the z-direction showing layers across HeLa cells. The pictures are taken from top to the bottom in a 2 μM distance. In these HeLa cells we were able to detect also some material taken up by these cells.
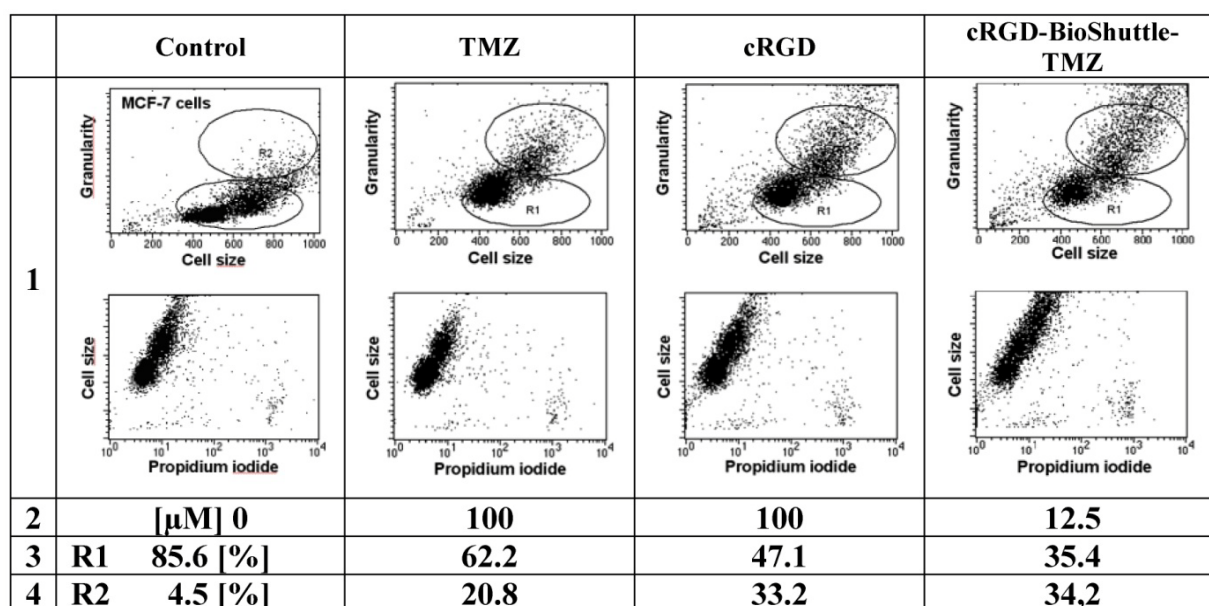
	Control	TMZ	cRGD	cRGD-BioShuttle-TMZ
1				
2	[μM] 0	100	100	12.5
3	R1 85.6 [%]	62.2	47.1	35.4
4	R2 4.5 [%]	20.8	33.2	34,2

Figure 5 the FACS analysis blots illustrate from left to right the effect of control TMZ, cRGD, and cRGD-BioShuttle-TMZ on the cell granularity (top row) and on the cell size (bottom row) of MCF-7 cells. As shown in the top row of the figure, the granularity differs from the untreated control and increases from the left (via TMZ and cRGD) to the right column (cRGD-BioShuttle-TMZ), whereas the cell size remains unaltered (as shown in the bottom row). The highest granularity is shown in the MCF-7 cells treated with the cRGD-BioShuttle-TMZ in an 8-fold reduced application dose (right column, top row). In comparison to the control (left column) the MCF-7 cells show an increased amount of a fraction of granularity cells (R2).

A comparison of the flow cytometry data (Table 1) to the CLSM data as shown in Figure 3 right column is useful. In the image of the 24 hours time point after application with cRGD-BioShuttle-dansyl the MCF-7 cells show a clear perinuclear endoplasmic reticular located blue fluorescence signal which represents an increase in the granularity resulting from the unstained endoplasmic reticulum surrounding the nucleus. As demonstrated in the Figure 5, second row, the cells treated with 100 μM TMZ show an increased amount of granular cells (20 %) compared to the untreated control with 4.5% granularity. In the sample of MCF-7 cells treated with the cRGD alone (100 μM), a cellular granularity of 33.2 % was measured. It is important to note that the MCF-7 cells treated with cRGD-BioShuttle-TMZ in an at least 8-fold reduced application dose (12.5 μM) feature the highest cell response with a cellular granularity of 34.2%.

Cellular sensitivity against cRGD, cRGD-BioShuttle-TMZ and TMZ alone - IC50 values

To measure the chemotherapeutic sensitivity against the investigated components, the TMZ, the cRGD, and the cRGD-BioShuttle-TMZ-conjugate were added to MCF-7 cells. Again, the substances were dissolved in an aqueous dilution series in culture medium in a concentration from 12.5 μM to 100 μM and applied over 72 hours. The data are presented in Table 1. With the flow cytometry analyses we showed the high sensitivity of MCF-7 against cRGD-BioShuttle-TMZ with an IC50 value of 12.5 μM, and a much lesser sensitivity against underivatized TMZ with an IC50 of 100 μM). The MCF-7 cells treated with cRGD (12.5 up to 100 μM) were unimpressed.

Table 1 Effect of the temozolomide (TMZ), cRGD, and cRGD-BioShuttle-TMZ on the MCF-7 breast cancer cell line.

	TMZ	cRGD	cRGD-BioShuttle
IC50 [μMol/L]	100	-	12.5
pIC50	4	-	4.9

Discussion

As definitive treatments of metastases of breast cancer remain surgery, radiation therapy, and hormone therapy in the case of metastatic progress. Cytogenetic characteristics, like the range of the chro-

mosome number between hypertriploidy and hypo-tetraploidy, could answer the question of the recalcitrance of metastatic breast cancer cells, exemplarily MCF-7 cells, against therapeutic interventions. But the timing of treatment for all stages of the disease remains controversial and new therapeutic approaches are needed [15, 16]. Encouraging results of the chemotherapeutic TMZ treatment in brain tumors [17] remain unendorsed in the treatment of breast cancer cells.

A May 28th 2010 search in the NCBI database PubMed with "RGD" "MCF-7" yields 26, and with "RGD" "HeLa" 89 hits. In its first 1995 publication the Huang group described inhibiting features of RGD-containing peptides against $\alpha_v\beta_3$ integrin expressing cells [18] whereas the activity of $\alpha_v\beta_5$ integrin was already documented from the Boulanger and Nemerow groups in 1993 [19, 20].

An explanation is that the integrin $\alpha_v\beta_3$ receptor is expressed at low levels in epithelial and mature endothelial cells but is upregulated on tumor cells and tumor endothelial cells of varying tumor types including breast cancer, and therefore became considered as a prognostic factor in breast cancer [21]. It was also documented that peptide ligands containing RGD amino acid sequences have a high affinity for integrins and after labelling with radioisotopes, could be used for imaging $\alpha_v\beta_3$ receptor levels by PET or SPECT studies [22]. The use of RGD peptides ligated with imaging components for cell specific targeting as tumor-diagnosing tool is broadly documented [23, 24]. All these documented radioligands may be valuable for monitoring antiangiogenic therapeutics. The ligation of such therapeutically active substances to RGD peptides could open a door for successful treatment of hardly tractable tumors like metastases expressing $\alpha_v\beta_3$ integrin. In comparison with the normal expression level of MCF-7 mammary cancer cells, $\alpha_v\beta_3$ low expressing HeLa cervix cancer cells were examined, which express the $\alpha_v\beta_5$ integrin and correlate with low invasiveness.

In flow cytometry, the increased relative amount of cells revealing granularity and the accession of the cell fraction featuring a clear augmentation of the granularity both might result from increased numbers of affected mitochondria, golgi apparatus or endoplasmatic reticulum. This could be explained with a pharmacologic effect of the cRGD, as well as of the TMZ alone. The BioShuttle construct containing the cRGD as targeting modul connected to the TMZ via the Diels-Alder Reaction with inverse electron demand [12] targets the $\alpha_v\beta_3$ and $\alpha_v\beta_5$integrin MCF-7 cell surface proteins as shown in the Figure 3. According to CLSM-pictures of the MCF-7 cells (Figure 3), an increased cytoplasmic coloring is indicative for a strongly increased amount of granularity in cells (R2) in the cytometric results. It is important to note that no changes in cell size could be observed.

The results of the present study demonstrate a close relationship of the reformulated drug to unanswered clinical questions as suitable solutions for the patients (as described in the introduction). Here we ligated TMZ to the cRGD, a peptide-based component, which accumulates at the cell's membrane surface holding a tremendous potential to optimize therapy. Enhanced local concentrations of active substances like TMZ at the cells surface, a feasible site of pharmacological action, allow expecting lower application doses with concomitantly decreased side-effects. The uptake and internalization into the cells cytoplasm is presumably documented [25]. The criteria to determine the applicability for targeting including accessibility, specificity, safety and subcellular precision are documented [26-30]. In order to fulfill all these biomedical aspects, the TMZ drug was bound as a cargo to transporter molecules (cRGD-BioShuttle-TMZ) with special chemical methods [31]. These coupling reactions however, required the reformulation of the active drug TMZ and can lead to novel properties of the TMZ. Chemoselective reaction-conditions in aqueous solution and at room temperature were obtained by chemical ligation of functional peptides via the DAR$_{inv}$. The "click chemistry" based on the DAR$_{inv}$ with "inverse electron demand" resulted in an impressive efficiency as illustrated in scheme 3/Figure S3 and is well documented [12]. This reaction enhanced the economics of the chemical reaction by the following parameters: ① increase of the reaction rate, ② gentle reaction conditions at room temperature, and ③ resulting in reaction kinetics with stoichiometric reaction partners without excess of the educts. The BioShuttle-mediated delivery and targeting platform can facilitate the transport to target cells [31, 32]. Despite the fact that the IC50 value can vary, depending on factors like the cell line, the test protocol, and the investigator, this estimation gives useful and helpful information on the relative toxicity [32]. Regarding the difference in IC50 values between the TMZ at 100 μmol/L and cRGD-BioShuttle-TMZ at 12.5 μmol/L, it becomes obvious that the cRGD-BioShuttle-TMZ offers a high potential for treatment of patients and represents an attractive enhanced drug system for upcoming clinical combined chemotherapeutic approaches [33, 34].

Conflict of Interest

The authors have declared that no conflict of interest exists.

References

1. NIH Consensus Statement. Breast cancer screening for women ages 40-49. NIH Consens Statement. 1997; 15: 1-35.
2. Harms JF, Welch DR, Samant RS, et al. A small molecule antagonist of the alpha(v)beta3 integrin suppresses MDA-MB-435 skeletal metastasis. Clin Exp Metastasis. 2004; 21: 119-28.
3. Takada Y, Ye X, Simon S. The integrins. Genome Biol. 2007; 8: 215.
4. Sakamoto S, Kyprianou N. Targeting anoikis resistance in prostate cancer metastasis. Mol Aspects Med. 2010 Apr;31(2):205-14.
5. Zanardi LA, Battistini L, Burreddu P, et al. Targeting alpha(v)beta(3) Integrin: Design and Applications of Mono- and Multifunctional RGD-Based Peptides and Semipeptides. Curr Med Chem. 2010;17(13):1255-99.
6. Chen X, Sievers E, Hou Y, et al. Integrin alpha v beta 3-targeted imaging of lung cancer. Neoplasia. 2005; 7: 271-9.
7. Willmann JK, Lutz AM, Paulmurugan R, et al. Dual-targeted contrast agent for US assessment of tumor angiogenesis in vivo. Radiology. 2008; 248: 936-44.
8. Liu Z, Niu G, Wang F, et al. (68)Ga-labeled NOTA-RGD-BBN peptide for dual integrin and GRPR-targeted tumor imaging. Eur J Nucl Med Mol Imaging. 2009; 36: 1483-94.
9. Haier J, Goldmann U, Hotz B, et al. Inhibition of tumor progression and neoangiogenesis using cyclic RGD-peptides in a chemically induced colon carcinoma in rats. Clin Exp Metastasis. 2002; 19: 665-72.
10. Oba M, Fukushima S, Kanayama N, et al. Cyclic RGD peptide-conjugated polyplex micelles as a targetable gene delivery system directed to cells possessing alphavbeta3 and alphavbeta5 integrins. Bioconjug Chem. 2007; 18: 1415-23.
11. Wiessler M, Kliem C, Lorenz P, Mueller E, and Fleischhacker H. EU Patent: Ligation reaction based on the Diels Alder Reaction with invers electron demand. [EP 06 012 414.6]. 6-10-2006.
12. Wiessler M, Waldeck W, Kliem C, et al. The Diels-Alder-reaction with inverse-electron-demand, a very efficient versatile click-reaction concept for proper ligation of variable molecular partners. Int J Med Sci. 2009; 7: 19-28.
13. Arrowsmith J, Jennings SA, Clark AS, et al. Antitumor imidazotetrazines. 41. Conjugation of the antitumor agents mitozolomide and temozolomide to peptides and lexitropsins bearing DNA major and minor groove-binding structural motifs. J Med Chem. 2002; 45: 5458-70.
14. Reppe W, Schlichting O, Klager K, et al. Cyclisierende Polymerisation von Acetylen I. Justus Liebigs Annalen der Chemie. 1948; 560: 1-92.
15. Chay C, Smith DC. Adjuvant and neoadjuvant therapy in prostate cancer. Semin Oncol. 2001; 28: 3-12.
16. Hegeman RB, Liu G, Wilding G, et al. Newer therapies in advanced prostate cancer. Clin Prostate Cancer. 2004; 3: 150-6.
17. Newlands ES, Blackledge GR, Slack JA, et al. Phase I trial of temozolomide (CCRG 81045: M&B 39831: NSC 362856). Br J Cancer. 1992; 65: 287-91.
18. Chang MC, Wang BR, Huang TF. Characterization of endothelial cell differential attachment to fibrin and fibrinogen and its inhibition by Arg-Gly-Asp-containing peptides. Thromb Haemost. 1995; 74: 764-9.
19. Belin MT, Boulanger P. Involvement of cellular adhesion sequences in the attachment of adenovirus to the HeLa cell surface. J Gen Virol. 1993; 74 (Pt 8): 1485-97.
20. Wickham TJ, Mathias P, Cheresh DA, et al. Integrins alpha v beta 3 and alpha v beta 5 promote adenovirus internalization but not virus attachment. Cell. 1993; 73: 309-19.
21. Gasparini G, Brooks PC, Biganzoli E, et al. Vascular integrin alpha(v)beta3: a new prognostic indicator in breast cancer. Clin Cancer Res. 1998; 4: 2625-34.
22. Beer AJ, Haubner R, Sarbia M, et al. Positron emission tomography using [18F]Galacto-RGD identifies the level of integrin alpha(v)beta3 expression in man. Clin Cancer Res. 2006; 12: 3942-9.
23. Zitzmann S, Ehemann V, Schwab M. Arginine-glycine-aspartic acid (RGD)-peptide binds to both tumor and tumor-endothelial cells in vivo. Cancer Res. 2002; 62: 5139-43.
24. Haubner R, Weber WA, Beer AJ, et al. Noninvasive visualization of the activated alphavbeta3 integrin in cancer patients by positron emission tomography and [18F]Galacto-RGD. PLoS Med. 2005; 2: e70.
25. Zhang C, Jugold M, Woenne EC, et al. Specific targeting of tumor angiogenesis by RGD-conjugated ultrasmall superparamagnetic iron oxide particles using a clinical 1.5-T magnetic resonance scanner. Cancer Res. 2007; 67: 1555-62.
26. Muzykantov VR. Biomedical aspects of targeted delivery of drugs to pulmonary endothelium. Expert Opin Drug Deliv. 2005; 2: 909-26.
27. Braun K, Pipkorn R, Waldeck W. Development and Characterization of Drug Delivery systems for Targeting Mammalian Cells and Tissues: A Review. Curr Med Chem. 2005; 12: 1841-58.
28. Peer D, Karp JM, Hong S, et al. Nanocarriers as an emerging platform for cancer therapy. Nat Nanotechnol. 2007; 2: 751-60.
29. Lammers T, Hennink WE, Storm G. Tumour-targeted nanomedicines: principles and practice. Br J Cancer. 2008; 99: 392-7.
30. Davis ME, Chen ZG, Shin DM. Nanoparticle therapeutics: an emerging treatment modality for cancer. Nat Rev Drug Discov. 2008; 7: 771-82.
31. Burke PA, DeNardo SJ, Miers LA, et al. Cilengitide targeting of alpha(v)beta(3) integrin receptor synergizes with radioimmunotherapy to increase efficacy and apoptosis in breast cancer xenografts. Cancer Res. 2002; 62: 4263-72.
32. Cheng Y, Prusoff WH. Relationship between the inhibition constant (K1) and the concentration of inhibitor which causes 50 per cent inhibition (I50) of an enzymatic reaction. Biochem Pharmacol. 1973; 22: 3099-108.
33. Braun K, Peschke P, Pipkorn R, et al. A biological transporter for the delivery of peptide nucleic acids (PNAs) to the nuclear compartment of living cells. J Mol Biol. 2002; 318: 237-43.
34. Braun K, von Brasch L, Pipkorn R, et al. BioShuttle-mediated plasmid transfer. Int J Med Sci. 2007; 4: 267-77.